II International Conference on Particle-based Methods – Fundamentals and Applications
PARTICLES 2011
E. Oñate and D.R.J. Owen (Eds)

SIMULATING THE DYNAMIC BEHAVIOR OF DROPLET IN A GROOVED CHANNEL BY DISSIPATIVE PARTICLE DYNAMICS

M. K. ZHANG[*], S. CHEN[*#] AND Z. SHANG[†]

[*] School of Aerospace Engineering and Applied Mechanics
Tongji University
Siping Road No. 1239, 200092 Shanghai, P. R. China
[#]corresponding author, e-mail: schen_tju@mail.tongji.edu.cn

[†] Science and Technology Facilities Council
Daresbury Laboratory
Warrington WA4 4AD, UK

Key words: Droplet, Wall Wettability, Contact Angle, Grooved Microchannel, Dissipative Particle Dynamics.

Abstract. In this paper, an improved dissipative particle dynamics (DPD) method was applied to simulate droplet motion in a grooved microchannel. Firstly the static contact angle between the droplet and the solid wall was simulated with the improved potential function, and "static contact angle~a_{wf}/a_f" curve was obtained by Polynomial Fit of the 2nd order. Then the influences of wall wettability, flow field force on the flow pattern of droplet were investigated in a grooved microchannel. The results show that wall wettability and flow field force have large effects on the flow pattern of the droplet.

1 INTRODUCTION

In the past decade, a variety of concepts has been developed for the construction of microfluidic system. For example, Yun et al.[1] proposed a micropump actuated by surface tension based on continuous electrowetting, this kind of micropump has achieved comparable performance to previous micropumps operated by various actuation mechanisms with extremely low power consumption and low voltage operation and can be used in application fields such as handheld micro lab-on-a-chips and portable biomedical devices where large pump pressure is not required. Gordillo et al. [2] presented a new method for the production of bubble-liquid suspensions composed of micro-sized bubbles. Using computer simulations, Kuksenok et al. [3] investigated the behavior of an immiscible binary AB fluid that is driven to flow through a microchannel, which is decorated with a checkerboard pattern of chemically distinct A- and B-like patches on the top and bottom walls. The results provided guidelines for designing microfluidic devices that can be used to effectively intermix multicomponent fluids. The development of microfluidic system usually requires understanding the mechanism of fluid flows, involving in various wetting, capillary phenomenon and fluid flow behaviors with free surfaces.

Many researches have demonstrated that roughness may apparently increase the hydrophobicity or hydrophilicity of the surface. Seemann et al.[4] reported even relatively

simple surface topographies such as grooves with rectangular cross section exhibit a large variety of different wetting morphologies. Mchale et al. [5] investigated topography driven spreading. Their results showed roughening a hydrophobic surface enhances its nonwetting properties into superhydrophobicity, and topographic effects can also enhance partial wetting by a given liquid into complete wetting to create superwetting. Huang et al. [6] studied a droplet moving inside a grooved channel by using a new lattice Boltzmann model for multiphase flows with large density ratio. The impacts of the adhesion and geometrical properties of the surface on the flow pattern and droplet velocity have been explored in detail.

The purpose of the present study is to obtain numerical simulation results for droplet motion in a grooved channel by dissipative particle dynamics. A modified particle-particle interaction potential with a combination of short-range repulsive and long-range attractive interaction is adopted to achieve vapor-liquid coexistence, and it could be used to simulate the flow behaviors of fluid with free surfaces. The effects of wall wettability and flow field force on the flow pattern of the droplet in a grooved microchannel have been discussed.

2 DISSIPATIVE PARTICLE DYNAMICS AND ITS MODIFICATION

Dissipative particle dynamics (DPD) is a mesoscale fluid simulation method proposed by Hoogerbrugge and Koelman[7]. The DPD model consists of particles representing molecular clusters, interacting with each other via conservative, dissipative, and random forces. Because the interaction between clusters of molecules is much softer than molecule-molecule interaction, longer time steps than MD could be taken in DPD.

In DPD system, the motion of each particle having position $\boldsymbol{r}_i$ and velocity $\boldsymbol{v}_i$ is governed by the kinematic theory $\mathrm{d}\boldsymbol{r}_i/\mathrm{d}t = \boldsymbol{v}_i$ and Newton's second law $\mathrm{d}\boldsymbol{v}_i/\mathrm{d}t = \boldsymbol{F}_i$, here the mass of each particle is taken as unit. Besides external force, the force $\boldsymbol{F}_i$ could be decomposed into conservative, dissipative and random components:

$$\boldsymbol{F}_i = \sum_{j\neq i}(\boldsymbol{F}_{C,ij} + \boldsymbol{F}_{D,ij} + \boldsymbol{F}_{R,ij}) \tag{1}$$

In formula (1), the distance between the two particles determines the magnitude of the conservative force $\boldsymbol{F}_{C,ij}$. The dissipative component $\boldsymbol{F}_{D,ij}$ is used to model viscosity of fluids while the random one $\boldsymbol{F}_{R,ij}$ compensates the kinetic energy reduced by dissipative force.

The conservative force usually takes the form:

$$\boldsymbol{F}_{C,ij} = a_{ij} w_C(r_{ij}) \hat{\boldsymbol{r}}_{ij} \tag{2}$$

where $w_C(r_{ij})$ is the weight function; a_{ij} is the interaction strength, which is the main parameter that models the local hydrostatic pressure in fluids; $\boldsymbol{r}_{ij} = \boldsymbol{r}_i - \boldsymbol{r}_j$, $r_{ij} = |\boldsymbol{r}_{ij}|$, and $\hat{\boldsymbol{r}}_{ij} = \boldsymbol{r}_{ij}/|\boldsymbol{r}_{ij}|$.

In conventional DPD, the conservative force weight function is a pure repulsive function:

$$w_C(r_{ij}) = (1 - r_{ij}/r_c) \tag{3}$$

here r_c is the cutoff radius, meaning that $w_C(r_{ij})$ vanishes for $r > r_c$. For more details, please see reference [8]. Conventional DPD particles interact with each other via soft interaction, leading to the apparent absence of a ρ^3 term in the equation of state, which can't produce vapor-liquid coexistence [9]. To deal with this difficulty, Pagonabarraga and Frenkel [10] developed a multibody DPD (MDPD), in which the conservative interaction depends on the

instantaneous local particle density. Using MDPD model or its modified versions, Warren [11,12] and Tiwari [13] et al. simulated kinds of phenomena such as vapor-liquid interface, oscillation of a cylindrical drop etc. Liu [14,15] introduced a new method with a combination of short range repulsive and long range attractive interaction to explore the potential of simulating the vapor-liquid coexistence and free surface phenomena.

In order to simulate the vapor-liquid coexistence or flow phenomena of liquids with free surface, in the present study the combination of short range repulsive and long range attractive interaction proposed by Liu [14,15] was applied to modify the conservative force, i.e. purely repulsive interaction, of the conventional DPD model. This new interaction potential is constructed by a linear combination of cubic spline which is often used in smoothed particle hydrodynamics (SPH), with different cutoff radius. The most commonly used smoothing function in SPH[16] is the cubic spline:

$$W(r) = W(r, r_c) = \begin{cases} 1 - \frac{3}{2}\left(\frac{2r}{r_c}\right)^2 + \frac{3}{4}\left(\frac{2r}{r_c}\right)^3 & 0 \le \frac{2r}{r_c} < 1 \\ \frac{1}{4}\left[2 - \left(\frac{2r}{r_c}\right)\right]^3 & 1 \le \frac{2r}{r_c} < 2 \\ 0 & \frac{2r}{r_c} \ge 2 \end{cases} \tag{4}$$

Our new interaction potential takes the form:

$$U(r) = a[AW(r, r_{c1}) - BW(r, r_{c2})] \tag{5}$$

here $W(r, r_{c1})$, $W(r, r_{c2})$ are cubic splines; r_{c1}, r_{c2} are different cutoff radius; A and B are coefficients which could be adjusted simply to modify different long range attractive interaction; a is the interaction strength. The DPD conservative force is obtained by taking the gradient of the new potential:

$$\boldsymbol{F}_{C,ij} = -\frac{dU(r)}{dr}\hat{\boldsymbol{r}}_{\boldsymbol{ij}} = -a[AW'(r, r_{c1}) - BW'(r, r_{c1})]\hat{\boldsymbol{r}}_{\boldsymbol{ij}} \tag{6}$$

For the choice of parameters, one case of interaction potential frequently used in this paper is:

$$U(r) = 18.75[2.0W(r, 0.8) - W(r, 1.0)] \tag{7}$$

which could achieve liquid-gas density ratio larger than 600, and could be used to approximately simulate the flow flows with free surfaces[14].

3 RESULTS AND DISSCUSSION

3.1 Simulation of static contact angle

The solid wall is represented by using frozen particles in the present study. Near the wall a thin layer is assumed where the no-slip boundary condition holds. A random velocity distribution is enforced in this layer with zero mean corresponding to a given temperature. Similar to the reflection law of Revenga et al. [17], we further require that particles in this layer always leave the wall. The velocity of particle *i* in the layer is

$$\boldsymbol{v}_i = \boldsymbol{v}_R + \boldsymbol{n}(\sqrt{(\boldsymbol{n} \cdot \boldsymbol{v}_R)^2} - \boldsymbol{n} \cdot \boldsymbol{v}_R) \tag{8}$$

where $\boldsymbol{v}_R$ is the reandom vector and $\boldsymbol{n}$ is the unit vector normal to the wall and pointing to the fluid. For more details, please see reference [18].

The webtabilly could be adjusted from hydrophobicity to hydrophilicity by changing the ratio of a_{wf}/a_f. Fig. 1 shows three different cases, in which the static contact angle is from 103° to 54°. With the increase of ratio a_{wf}/a_f , the attractive force betwen the wall particles and the fluid particles is strengthened, the static contact angle becomes smaller.

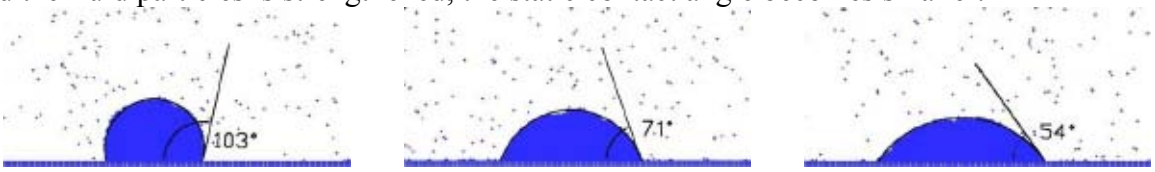

(a) $k_BT = 1.0$, $a_{wf}/a_f = 0.707$ (b) $k_BT = 1.0$, $a_{wf}/a_f = 1.0$ (c) $k_BT = 1.0$, $a_{wf}/a_f = 1.225$

Figure 1: Static contact angles for different ratio of a_{wf}/a_f

The "static contact angle~a_{wf}/a_f" relation is obtained by Polynomial Fit of the 2nd order, described as

$$\theta = 20.202(a_{wf}/a_f)^2 - 129.71(a_{wf}/a_f) + 181.61 \quad (9)$$

Accordingly, the relation curve between a_{wf}/a_f and static contact angle is shown in Figure 2.

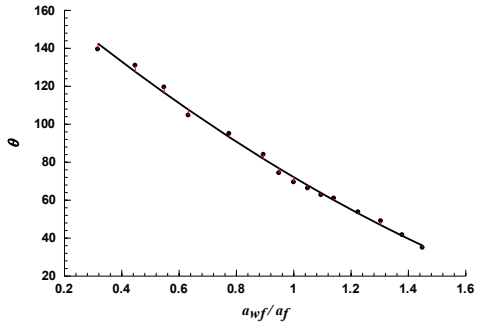

Figure 2: Relation curve between a_{wf}/a_f and static contact angle

3.2 Simulation of droplets motion in grooved microchannel

3.2.1 Effect of wall wettability

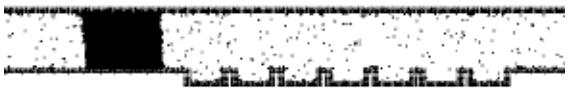

Figure 3: A droplet in a grooved microchannel

The computational domain consists of three phases: droplet, vapor and solid wall of the channel, as shown in Fig. 3. The lower wall of the channel is roughened by grooves. The size of the channel is $120 \times 10 \times 16$, while the size of the grooves is set as 7×3 and the size of the protuberant part is 3×3. There are totally 37760 DPD particles in the computational domain, in which the wall and the fluid are made up of 16960 and 20800 particles, respectively. The initial configurations of fluid and wall particles are generated by a pre-processing program and read in as input data. The initial velocities of the fluid particle are set

randomly according to the given temperature, while the wall particles are frozen. Periodic boundary conditions are applied on the flow boundaries of the computational domain in the X and Y directions.

From the Polynomial Fitting curve as shown in Fig. 2 we can see that the static contact angles of 130°, 110°, 90°, 70° and 50° correspond to the ratios of a_{wf}/a_f from 0.426, 0.610, 0.808, 1.024 to 1.263, respectively, Similar to reference [6]. The upper wall is kept neutral-wetting (i.e. $\theta = 90°$), while the lower contact angles are adjusted from hydrophobicity to hydropholicity.

Using the improved weight function, vapor-liquid coexistence could be reached. The parameters a, A, r_{c1}, r_{c2} are set as in Equation (7), so liquid-gas density ratio of larger than 600 could be obtained [14]. At the beginning of the simulation the particles are allowed to move without applying the external force until the thermodynamic equilibrium state is reached. Then the external force field of $g = 0.01\sqrt{2}, \alpha_F = -45°$ is applied to fluid particles and the nonequilibrium simulation starts. Fig. 5 shows the snapshots of the droplet motion under different wettability. With the increase of the hydropholicity, the drag acted on the droplet increases, the flow velocity of the droplet becomes smaller, which is in agreement with the simulation results of reference [6] by LB method.

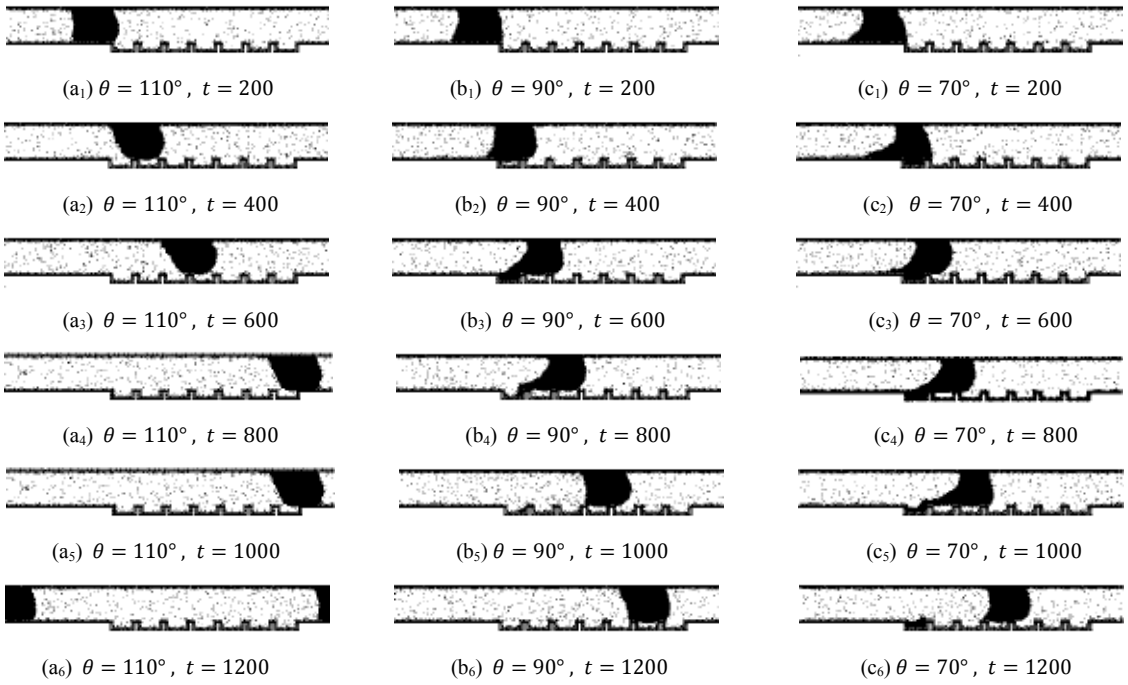

Figure 5: Snapshots of the droplet motion under different wettability

Fig. 6 shows the comparison of droplet motion velocity under different wetting conditions. The droplet repeats the motion mode of "contact with one protuberant part" and "contact with two protuberant parts". When the droplet contacts with one protuberant part, the contact area decreases, and the drag force decreases. Accordingly, the droplet velocity increases. While the droplet contacts with two protuberant parts, the contact area increases, and the drag force increases. Accordingly, the droplet velocity decreased. Hence it is noted that velocity fluctuation exists when the droplet move forward from Fig 6.

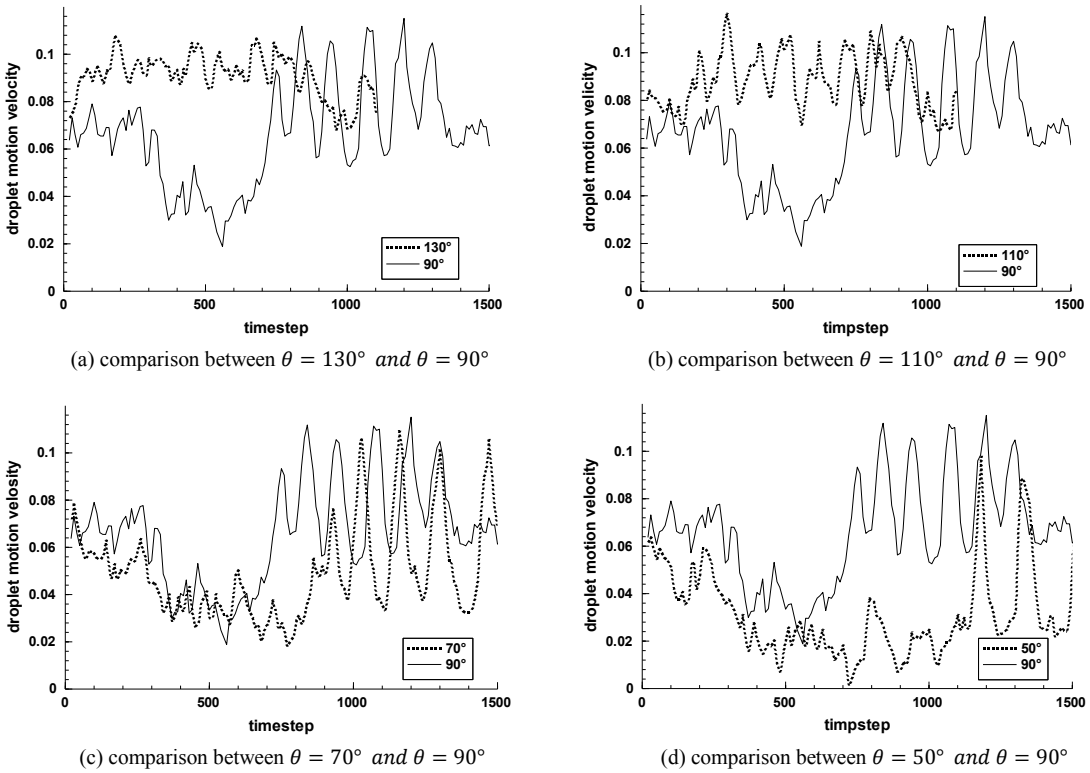

(a) comparison between $\theta = 130°$ and $\theta = 90°$ (b) comparison between $\theta = 110°$ and $\theta = 90°$

(c) comparison between $\theta = 70°$ and $\theta = 90°$ (d) comparison between $\theta = 50°$ and $\theta = 90°$

Figure 6: Comparison of droplet velocity under different wetting conditions

3.2.2 Effects of external force direction

In this section, the effects of external force direction on the droplet motion are investigated by keeping the horizontal component of exerrnal force fixed and changing the vertial component. The upper and lower walls are kept neutral wetting, two kinds of external force directions are applied: ① $\alpha_F = 45°$ ($g_x = 0.01$， $g_z = -0.01$) and ② $\alpha_F = 0°$ ($g_x = 0.01$， $g_z = 0$). Fig. 7 shows the different dynamic behaviors of droplet motion in flat plate channel under different extarnal force directions.

(a) $t = 230$, $\alpha_F = 45°$ (b) $t = 230$, $\alpha_F = 0°$

Figure 7: Comparison of droplet motion under different extrnal force directions

Then we simulate the dynamic behavors of droplet in grooved channels. Three kinds of external force directions are applied: ① $\alpha_F = 45°$ ($g_x = 0.01$， $g_z = -0.01$), ② $\alpha_F = 30°$ ($g_x = 0.01$， $g_z = -0.00577$), ③ $\alpha_F = 0°$ ($g_x = 0.01$， $g_z = 0$). Fig. 8 shows comparison of snapshos of droplet motion under different external force directions. As can be seen from Fig. 8, the contact area between the droplet and the protuberant parts of the lower wall increases with the increase of α_F. The smaller the downward component of field force is, the faster the droplet flows in the microchannel.

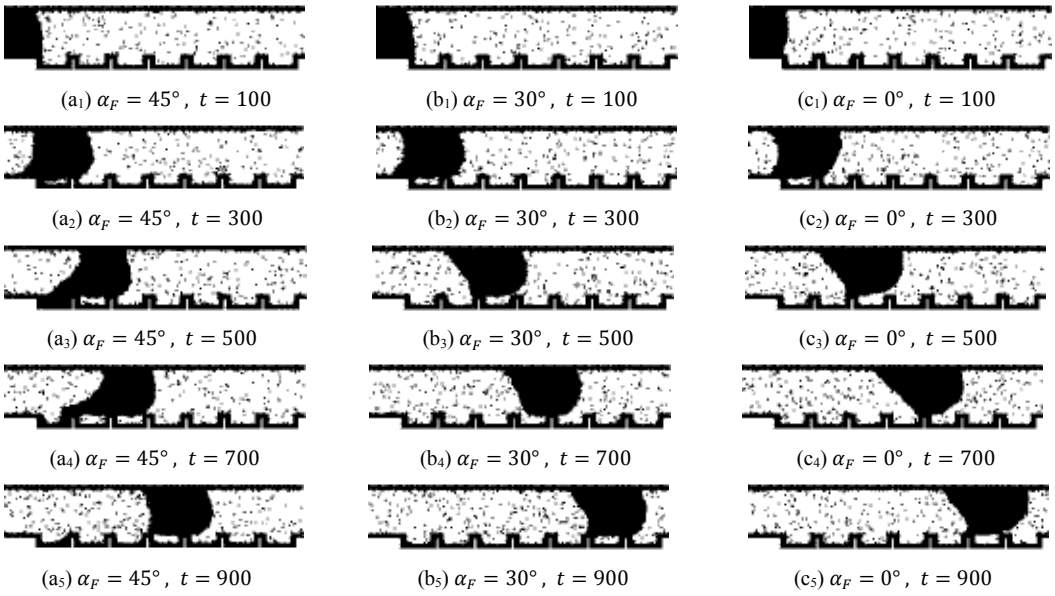

Figure 8: Comparison of snapshos of droplet motion under different external force directions

Fig. 9 shows the comparison of droplet velocity under different external force directions. The vertical component of external force enhances the contact of the droplet on the wall, hence the velocity fluctuation of the droplet is enlarged when the vertical component is increased.

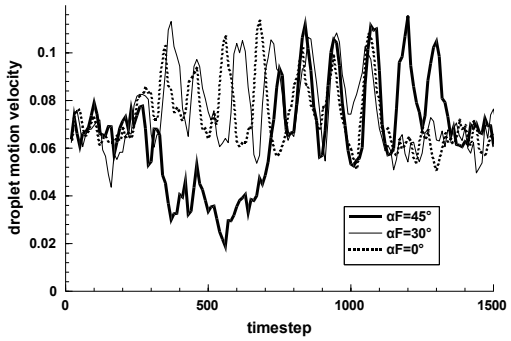

Figure 9: Comparison of droplet velocity under different external force directions

4 CONCLUSIONS

In the present study, a modified DPD method with a combination of short-range repulsive and long-range attractive interaction is adopted to investigate the dynamic behaviors of droplet in a grooved channel. The results show that the wettability of wall and external force direction significantly affect the dynamic behaviors of droplet in grooved channel. The motion velocity of the droplet decreased with the increase of the wettability. There exists velocity fluctuations when the droplets move inside a grooved channel, and the magnitude of the velocity fluctuations is related to the wetting conditions and the vertical component of the external force. This study is helpful to understand the fluid flow behavior with free surface on rough surfaces.

REFERENCES

[1] Yun, K.S., Cho, I.J, Bu, J.U. and Kim, C.J. A surface-tension driven micropump for low-voltage and low-power operations. *Journal of Microelectromechanical Systems* (2002) **11**: 454-461.

[2] Gordillo, J.M., Cheng, Z.D., Ganan-Calov, A.M., Marquez, M. and Weitz, D.A. A new device for the generation of microbubbles. *Physics of Fluids* (2004) **16**: 2828-2834.

[3] Kuksenok, O. and Balazs, A.C. Simulating the dynamic behavior of immiscible binary fluids in three-dimensional chemically patterned microchannels. *Physical Review E* (2003) **68**: 011502.

[4] Seemann, R., Brinkmann, M., Kramer, E.J., Lange, F.F and Lipowsky, R. Wetting morphologies at microstructured surfaces. *PNAS* (2005) **102**: 1848-1852.

[5] McHale, G., Shirtcliffe, N.J., Aqul, S., Perry, C.C. and Newton, M.I. Topography driven Spreading. *Physical Review Letters* (2004) **93**: 036102.

[6] Huang, J.J., Shu, C. and Chew, Y.T. Lattice Boltzmann study of droplet motion inside a grooved channel. *Physics of Fluids* (2009) **21**:022103.

[7] Hoogerbrugge, P.J. and Koelman, J.M.V.A. Simulating microscopic hydrodynamic phenomena with dissipative particle dynamics. *Europhys. Lett.* (1992) **19:**155-160.

[8] Chen, S., Phan-Thien, N., Fan, X.J. and Khoo, B.C. Dissipative particle dynamics simulation of polymer drops in a periodic shear flow. *J. Non-Newtonian fluid Mech.* (2004) **118**: 65-81.

[9] Groot, R.D. and Warren, P.B. Dissipative particle dynamics: bridging the gap between atomistic and mesoscopic simulation, *J. Chem. Phys.* (1997) **107**: 4423-4435.

[10] Pagonabarraga, I. and Frenkel, D. Dissipative particle dynamics for interaction system. *J. Chem. Phys* (2001) **115**:5015-5021.

[11] Warren, P.B., Hydrodynamic Bubble coarsening in off-critical vapor-liquid phase separation. *Phys. Rev. Lett.* (2001) **87**: 225702.

[12] Warren, P.B. Vapor-liquid coexistence in many-body dissipative particle dynamics, *Phys. Rev. E* (2003) **68**: 066702.

[13] Tiwari, A. and Abraham, J. Dissipative-particle-dynamics model for two-phase flows. *Physical review E*, (2006) **74**: 056701.

[14] Liu, M.B., Meakin, P. and Huang, H. Dissipative particle dynamics with attractive and repulsive particle-particle interacdtions. *Physics of Fluids* (2006) **18**: 017101.

[15] Liu, M.B., Meakin, P. and Huang, H. Dissipative particle dynamics simulation of multiphase fluid flow in microchannels and microchannel networks. *Physics of Fluids* (2007) **19**: 033302.

[16] Liu, M. B., Liu, G. R., Lam, K.Y. Constructing smoothing functions in smoothed particle hydrodynamics with applications. *J. Comput. Appl. Math.* (2003) **155**: 263-269.

[17] Revenga, M., Zuniga, I. and Espanol. P. Boundary models in DPD. *Int. J. Mod. Phys. C* (1998) **9**:1319-1323.

[18] Fan, X.J., Phan-Thien, N., Ng, T.Y., Wu, X.H. and Xu, D. Microchannel flow of a macromolecular suspension. *Physics of Fluids* (2003) **15**:11-21.